Antibacterial activity of silver and titania nanoparticles on glass surfaces

Kummala, Ruut; Brobbey, Kofi; Haapanen, Janne; M Mäkelä, Jyrki; Gunell, Marianne; Eerola, Erkki; Huovinen, Pentti; Toivakka, Martti; J Saarinen, Jarkko

Published in:
Advances in Natural Sciences: Nanoscience and Nanotechnology

DOI:
10.1088/2043-6254/ab0882

Publicerad: 01/01/2019

Document Version
(Referentgranskad version om publikationen är vetenskaplig)

Antibacterial activity of silver and titania nanoparticles on glass surfaces

Ruut Kummala[a], Kofi J. Brobbey[a], Janne Haapanen[b], Jyrki M. Mäkelä[b], Marianne Gunell[c,d], Erkki Eerola[c,d], Pentti Huovinen[c,d], Martti Toivakka[a], and Jarkko J. Saarinen[e]

[a] Laboratory of Paper Coating and Converting, Center for Functional Materials at Biological 5 Interfaces (FUNMAT), Abo Akademi University, Porthaninkatu 3, FI-20500 Turku, Finland

[b] Aerosol Physics Laboratory, Department of Physics, Tampere University of Technology, P.O. 7 Box 692, FI-33101 Tampere, Finland

[c] Department of Medical Microbiology and Immunology, University of Turku, Kiinamyllynkatu 9 13, FI-20520 Turku, Finland

[d] Department of clinical microbiology and immunology, Turku University Hospital, 11 Kiinamyllynkatu 13, FI-20520 Turku, Finland

[e] Department of Chemistry, University of Eastern Finland, P.O. Box 111, FI-80101 Joensuu, Finland

Email : jarkko.j.saarinen@uef.fi

Abstract. A liquid flame spray (LFS) nanoparticle deposition process was used to generate glass surfaces with silver (Ag) and titania (TiO_2) nanoparticles for antibacterial activity against two common pathogenic bacteria causing community-associated and hospital-acquired infections, gram positive *Staphylococcus aureus* (*S. aureus*) and gram negative *Escherichia coli* (*E. coli*). All nanoparticle coatings increased antibacterial activity compared to a reference glass surface. The silver nanoparticle coatings showed the highest antibacterial activity with *E. coli*. On contrary, TiO_2 nanoparticle coatings were found to have a higher antibacterial activity against *S. aureus* than *E. coli*. No significant differences in antibacterial activity were observed between the two used nanoparticle deposition amounts.

Keywords: nanoparticle, antibacterial, glass, *E. coli*, *S. aureus*

Classification numbers: 2.00, 2.05, 4.00, 4.02, 5.08

1. Introduction

Hospital acquired infections (HAIs) are a quickly growing global problem with approximately 5 % of the hospitalized patients contracting HAI with the percentage raising up to 25–50 % for intensive care and severe cancer patients. In the United States only, the HAIs result in more than 2 million infections annually with significant morbidity and approximately 5 % mortality (up to 25 % at the intensive care units) [1]. This makes HAIs the fourth leading cause of deaths in the US killing more people than HIV and breast cancer combined. The annual direct costs of HAIs were estimated up to 35 billion USD in 2009 [1]. However,

the current estimate is significantly higher due to both increased treatment cost and existence of multiple drug resistant HAIs.

Antibacterial resistance is a worldwide concern as the conventional infection prevention and treatment methods against the common health-care associated and community acquired infections are becoming ineffective [2,3]. While new treatments are being developed, greater effort has been given to the prevention of infections by improved hygiene, infection control, and other prevention measures [4]. Such programs in hospitals were observed to decrease morbidity, improve survival rate, and shorten hospital stays while being cost-effective [5]. Recently, antibacterial surfaces were studied for infection control programs to passively stopping and slowing down the bacterial growth and transmission in hospital environment [6].

These examples reveal an urgent demand for effective tools to prevent bacterial infections especially in hospitals where surface hygiene is paramount. Metallic silver is well-known for its low toxicity to human cells but high toxicity to bacteria [7]. Alternatively, metallic copper alloys and copper surfaces were shown to reduce bacterial growth by 90 – 100 % compared to stainless steel surfaces [8].

Recent advances in nanoscale manufacturing tools have resulted in a wide use of nanoparticles and nanostructures in commercial applications including medicine. Surface modification of nanostructures can improve stability,

compatibility, and cell-selectivity of nanostructures [9]. Various metal (Ag) and metal oxide (ZnO, CuO, CeO_2, MgO, Fe_2O_3, AgO) nanoparticles have been studied for their antibacterial properties, and the mechanisms behind the antibacterial activity have been investigated [10-14]. Nanoparticles can be incorporated into bacteria by surface or intracellular uptake. In addition, metal ion leaching from nanoparticles can contribute to the nanoparticle antibacterial activity. Copper surfaces, for example, are highly reactive and toxic to bacteria as they can generate reactive oxygen species (ROS) such as superoxides on the intracellular level [15]. Antibacterial surfaces can be either bactericidal inactivating bacteria by chemical mechanisms [16] or bacteriostatic inhibiting the growth of bacteria [17].

In this paper we use a liquid flame spray (LFS) nanoparticle deposition on glass to induce effective and controllable antibacterial activity. LFS is a powerful tool for large-area deposition of nanoparticle functionalized surfaces that operates in atmospheric conditions with high material yield producing grams of nanomaterial per minute [18]. It is believed that nanoparticle surfaces with antibacterial activity will find many applications in the hospital environment in the future.

2. Experimental

2.1. *Liquid flame spray (LFS) nanoparticle synthesis and deposition*

An organometallic liquid precursor is injected directly into a turbulent H_2-O_2 -flame in which the precursor evaporates followed by nanoparticle formation via physical and thermochemical reactions [19]. The combustion gases produce a high temperature (max ~2 500°C) flame that can evaporate a wide variety of liquid precursors allowing also a generation of multi-component nanoparticle coatings [20]. LFS process is a high throughput and cost-effective method for nanoparticle deposition in the range of tens of mg/m_2 on surfaces. The LFS can be applied for coating large-area surfaces on various substrates either in a roll-to-roll process flow [21] or in a batch process depending on the application. Additionally, the LFS technology can easily be upscaled to the industrial level with roll-to-roll line speeds exceeding 300 m/min.

Silver (Ag) and titania (TiO_2) nanoparticles were deposited using LFS on glass surface. The LFS produced nanoparticles were deposited on the substrate surface through a tailor-made flow tube. A residual tube LFS deposition method was used *i.e.* the flame was pointed towards one end of a flow tube and the deposition was made from the other end of the tube onto the surface. Such an indirect procedure from the flame decreases the heat effects on the surface and enables a more uniformly distributed nanoparticle coating on a large area. Nanoparticles were

deposited on commercial microscope glasses (Menzel Gläser, Germany) with the following parameters: for Ag nanoparticles $AgNO_3$ (250 mg/ml, Alfa Aesar, 99.9 %) in deionized water was injected with a rate of 2 ml/min and for TiO_2 nanoparticles Ti(IV)isopropoxide (50 mg/ml, TTIP, Alfa Aesar, 97+ %) in 2-propanol (VWR, HPLC grade) was injected with a rate of 6 ml/min. The flame was formed mixing H_2 (40 standard liters per minute (slpm)) with O_2 (20 slpm). Two different nanoparticle amounts were utilized that were controlled by the deposition time *i.e.* 10 s and 60 s for low and high deposition amount, respectively. The effect of the heat from the flame on the glass surfaces was studied using a similar H_2-O_2 -flame but without the feed of precursor *i.e.* no nanoparticles were formed.

2.2. *Physico-chemical characterization of the nanoparticle glass surfaces*

The size and shape distribution of nanoparticles deposited by the indirect LFS were characterized using a scanning electron microscope (SEM, Jeol JSM-6335F). The samples were coated using a platinum sputtering for 15 s for conductivity. Energy-dispersive X-ray spectroscopy (EDS/EDX) was used together with the SEM to qualitatively determine particle compositions of the surfaces.

A contact angle (CA) goniometer KSV CAM 200 (KSV Instruments Ltd., FI). with a digital CCD camera having a 55 mm zoom microscope lens and a blue

LED light source was used to determine the water contact angle. A purified water drop (Milli-Q filtration, Millipore, US) with a volume of 4 µl was placed onto the surface from which static contact angles were measured at room temperature after 2 seconds from placing the drop. The mean contact angle was calculated from three to five parallel measurements on the sample surface with standard deviation.

Elemental composition of all the samples and oxidation stages of the nanostructures were analyzed by using an X-ray photoelectron spectroscopy (XPS, PHI Quantum 2000, Physical Electronics Instruments, US) with a monochromatic Al Kα X-ray source operated at 50 W with a take-off angle of 45°. Three measurements were used performed from each sample surface. Survey and high resolution spectra were acquired using an electron pass energy of 117.4 eV and 23.5 eV, respectively. The primary binding energy peaks of carbon and oxygen were collected for all samples. The corresponding metal (Ag and Ti) primary binding energy peaks and Auger peaks for Ag were acquired for nanoparticle coated samples. The pressure inside the main chamber was below 1.0×10^{-6} Torr during the spectra acquisition. Spectra were analysed with MultiPak V9.0.0 software (Ulvac-phi, Inc).

2.3. *Antibacterial activity testing*

Antibacterial activity of nanostructured surfaces was tested using a modified procedure developed by Pallavicini *et al.* [22] for *Staphylococcus aureus* (*S.*

aureus, Gram positive) ATCC 29213 and *Escherichia coli* (*E. coli*, Gram negative) ATCC 25922. Micro-organisms were grown overnight in a Luria-Bertani medium at 37°C. Cells were suspended to a phosphate buffered saline media until optical density at 600 nm (OD600) was approximately 0.1 corresponding to approximately 1×10^8 colony-forming units (CFU/ml). Bacterial suspension (10 µl) was then deposited onto the nanostructured microscope glass and a standard cover glass (24×24 mm^2) was set on top. Bacteria suspension formed a thin film between the nanostructured media and the cover glass. Subsequently glasses were transferred into a 50 ml Falcon test tube in which 1 ml of phosphate buffered saline (PBS) was pipetted to maintain damp environment. Two glass compilations were prepared for each bacteria strain, which were kept at a room temperature for 5 and 24 hours. After the determined contact period, 9 ml of PBS was added to the Falcon tube and shaken gently to detach the glass slides from each other. Sample suspension (10 µl) from Falcon tube was placed on an agar plate. The CFUs were counted after an overnight incubation from the agar plates.

3. Results

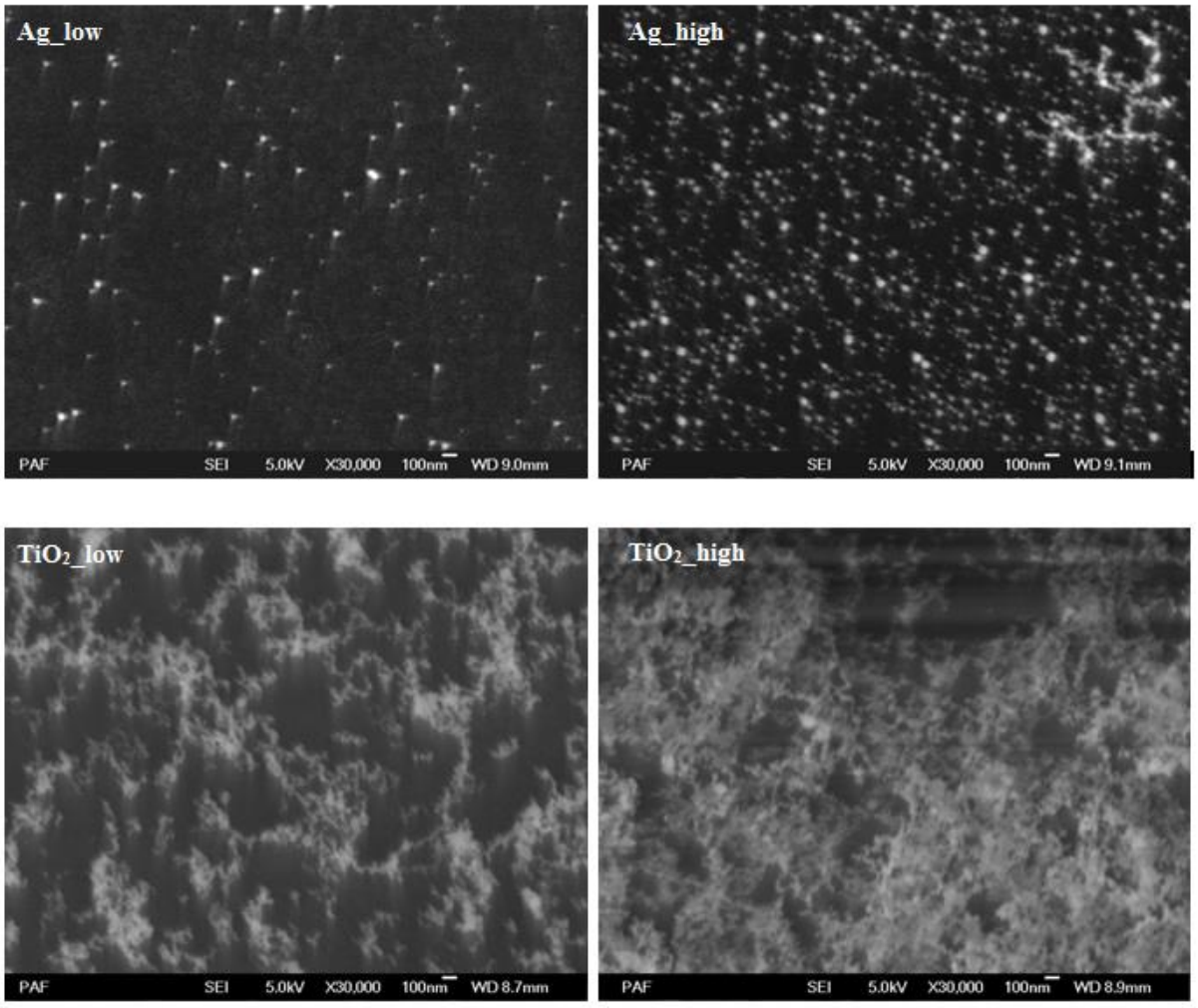

Figure 1. Nanoparticle coatings deposited by the indirect LFS on the microscope glass surfaces.

Figure 1 displays the SEM images of deposited Ag and TiO_2 nanoparticles that are rather evenly distributed on the glass surface. Nanoparticles in the sample Ag_low NPs were primarily individual particles whereas the Ag_high had more agglomerates. Individual silver nanoparticles had an average diameter of 35 nm.

TiO_2 nanoparticles were smaller in size and they were aggregated creating a porous structure.

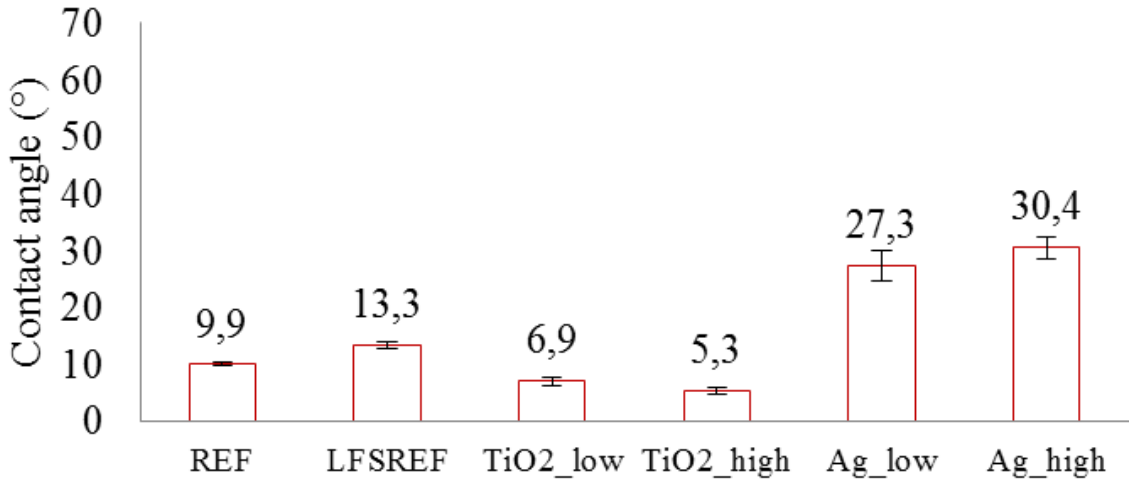

Figure 2. Water CAs of the nanostructured surfaces. The error bars are +/- standard deviations.

Surface hydrophilicity was verified using water CA measurement with deionized water at a room temperature. Figure 2 presents the average contact angles on the nanostructured sample surfaces together with a plain microscope glass surface. The water CA was increased for Ag nanoparticles whereas smaller water CA was observed for TiO_2 nanoparticles compared to the unmodified glass.

Table 1. Elemental composition of the used microscope slides and nanostructured surfaces with standard deviation (SD).

	Ag/Ti	SD	C	SD	O	SD	Si	SD	Na	SD
Ref	-	-	27.6	0.9	48.4	0.7	16.2	1.1	6.5	1.4
Flame	-	-	28.0	1.3	46.8	1.2	15.6	0.6	8.4	0.6
Ag_low	0.7	0.02	24.0	0.1	50.5	0.5	18.5	0.8	5.1	0.5
Ag_high	3.0	0.5	20.4	1.5	49.0	1.0	18.9	0.2	6.4	0.5
TiO_2_low	5.5	0.2	23.3	1.0	52.2	0.9	13.1	0.3	4.8	0.3
TiO_2_high	13.6	0.3	23.8	0.2	51.2	0.1	5.7	0.3	5.7	0.1

Table 1 presents the relative elemental composition of the sample surfaces analyzed using XPS. The components of glass, *i.e.*, silicon, oxygen, sodium, and small amounts of magnesium and calcium (in the range of 1% to 2%) were identified on all samples. The arbitrary carbon peak was used as a charge reference (284.8 eV) that is common for samples exposed to air due to contamination such as hydrocarbons. The results show that increasing the surface coating coverage decreases the atomic percentage of glass components that is due to the low XPS detection depth of 10 nm. Relative amounts of Ag or Ti increase with longer LFS deposition times as expected with a larger number of nanoparticles deposited on the surface.

Table 2. Primary binding energy, modified Auger parameter and spin-splitting of metal and metal oxide surfaces from XPS curves.

	Ag_low	Ag_high	TiO_2_low	TiO_2_high
Binding energy (eV)	367.9	367.9	457.9	458.0
Modified Auger parameter (eV)	725.9	725.9	-	-
Spin-splitting (eV)	-	-	5.7	5.7

Spin splitting and modified Auger parameter were used to determine metal oxidation primary binding energy state as presented in Table 2. Spin splitting of the primary titanium peaks was determined at 5.7 eV for both TiO_2_low and TiO_2_high, which corresponds to the characteristic value of 5.7 eV of TiO_2 in comparison to 6.1 eV of metallic Ti [23,24]. In literature, modified Auger parameters (A') of silver are 726.1 eV for metallic Ag, 724.5 eV for AgO, and 724.4 eV for Ag_2O [25]. For both Ag_low and Ag_high A' was 725.9 eV that is in agreement with metallic silver. Deconvolution of LFS deposited silver nanoparticles into Ag, AgO, and Ag_2O was presented in our previous study [26] that confirms the findings from the modified Auger parameter: more than 90% of silver was in metallic form Ag whereas Ag_2O and AgO contributed to less than 7% and 1%, respectively.

Table 3. Results of the antibacterial activity testing using semi-quantitative colony forming unit counting and untreated Menzel microscope glass as a reference.

	E. coli		*S. aureus*	
	5 h	24 h	5 h	24 h
Ref	+ / ++	+ / ++	+ / ++	+
Ag_low	-	-	- / +	1 CFU*
Ag_high	-	-	- / +	2 CFU*
TiO_2_low	+	+	+	- / +
TiO_2_high	+	+	+	- / +

*CFU = colony forming unit with + = 10^3 – 10^4, ++ = 10^4 – 10^5, and +++ > 10^5

A quantitative antibacterial activity test against *E. coli* and *S. aureus* was used to characterize the antibacterial properties of the nanostructured surfaces [22] with bacterial contact times of 5 and 24 hours. All nanostructured surfaces exhibited a lower bacterial growth at all time points compared to the reference microscope glass surface as shown in Table 3. Both silver coatings completely inhibited the growth of *E. coli* and decreased significantly the amount of viable *S. aureus*. It should also be noted that viable amount of *S. aureus* decreased on the reference glass surface from 5 h and 24 h contact time. Both TiO_2 surfaces exhibited a slightly lower growth of both bacteria. Additionally, enhanced antimicrobial

activity can be achieved by photocatalytic activation of TiO_2 nanoparticles with ultraviolet A (UVA, 315–400 nm) radiation. UVA radiation can generate electron-hole pairs, which can induce ROS on TiO_2 nanoparticle surface. These highly active ROS can interfere with the bacterial cell membrane in various ways depending on the experimental set-up, and photocatalytically activated TiO_2 surfaces have been demonstrated with improved antibacterial response [27,28]. We plan to return to this issue in a future communication.

4. Discussion

The indirect LFS nanoparticle deposition resulted in a relatively uniform nanoparticle coating with a simple control of the coating amounts by the deposition time. The adhesion of nanoparticles onto the surface takes place via van der Waals forces.

Elemental composition of the modified surface was dominant for the antibacterial activity of nanostructured glass surfaces. Variation on the amount of coatings did not have a significant effect on the antibacterial activity. All studied surfaces were hydrophilic, and the observed differences in surface wetting do not have a significant role in antibacterial activity. We have recently shown that even a change of surface wetting from hydrophilic to hydrophobic did not alter the antimicrobial activity against *E. coli* on plasma coated LFS deposited nanoparticles [29]. Toxicity mechanisms of nanoparticles are not completely

understood but reactive oxidative species and metal ions are the most commonly reported factors [30]. In literature Ag+ ion release has been suggested to be the only toxicity mechanism of Ag nanoparticles [31], which may be affected by the amount, size, and shape of the silver nanoparticles. It has also been proposed [32] that antibacterial activity of Ag nanoparticle coatings is mainly dependent on the total surface area of Ag nanoparticles that correlates to their potential for silver ion leaching.

5. Conclusions

In this study, silver and titania nanoparticle coated glasses were investigated for antibacterial activity against *E. coli* and *S. aureus* bacteria. It was shown that both Ag and TiO_2 nanoparticles can reduce bacterial growth on glass surface. Our results showed variations in the antibacterial activity of nanostructured surfaces depending on their chemical composition. In our study, the elemental composition of the nanostructured media was observed to be the most important factor for the antibacterial activity. The amount of metal and metal oxide together with the wettability of the coating did not have is significant effect on bacterial viability, even though they may have effect on bacteria adhesion to the substrate.

We believe that nanostructured antibacterial surfaces will find many applications in the future. Furthermore, development of bacterial resistance is less probable with nanostructured media compared to the conventional antibiotics

because such nanomaterials can attack a broad range of targets in the bacteria, for example, membrane proteins, lipid bilayer, and DNA damage by nanoparticle uptake.

Acknowledgments

This work was supported by the Academy of Finland under the project "Nanostructured large-area antibacterial surfaces (nLABS, grant no 275 475)". J. J. S. wishes to thank the UEF Faculty of Science and Forestry (Grant No. 579/2017) for the financial support.

References

[1] Scott RD 2009 *The direct medical costs of healthcare-associated infections in US hospitals and the benefits of prevention* Centers for Disease Control and Prevention.

[2] Levy SB and Marshall B 2004 *Nat. Med.* **10** S122.

[3] Bush K, Courvalin P, Dantas G, Davies J, Eisenstein B, Huovinen P, Jacoby GA, Kishony R, Kreiswirth BN, Kutter E, Lerner SA, Levy S, Lewis K, Lomovskaya O, Miller JH, Mobashery S, Piddock LJV, Projan S, Thomas CM, Tomasz A, Tulkens PM, Walsh TR, Watson JD, Witkowski J, Witte W, Wright G, Yeh P and Zgurskaya HI 2011 *Nat Rev Micro.* **9** 894.

[4] WHO 2014 *Antimicrobial Resistance: Global Report on Surveillance 2014* (World Health Organization, France).

[5] Sydnor ERM and Perl TM 2011 *Clin. Microbiol. Rev.* **24** 141.

[6] Otter JA 2013 *Healthc. Infect.* **18** 42.

[7] Clement JL and Jarrett PS 1994 *Metal-Based Drugs* **1** 467.

[8] Casey AL, Adams D, Karpanen TJ, Lambert PA, Cookson PD, Nightingale P, Miruszenko L, Shillam R, Christian P and Elliott TSJ 2010 *J. Hosp. Infect*. **74** 72.

[9] Kemp MM, Kumar A, Mousa S, Park T, Ajayan P, Kubotera N, Mousa SA and Linhardt RJ 2009 *Biomacromolecules* **10** 589.

[10] Gunawan C, Teoh WY, Ricardo, Marquis CP and Amal R, 2013 *Part. Part. Syst. Char.* **30** 375.

[11] Gunawan C, Teoh WY, Marquis CP and Amal R 2011 *ACS Nano* **5** 7214.

[12] Ting SRS, Whitelock JM, Tomic R, Gunawan C, Teoh WY, Amal R and Lord MS 2013 *Biomaterials* **34** 4377.

[13] Gokulakrishnan R, Ravikumar S and Raj JA 2012 *Asian Pac. J. Trop. Dis.* **2**

411.

[14] Negi H, Agarwal T, Zaidi MGH and Goel R 2012 *Ann. Microbiol.* **62** 765.

[15] Macomber L and Imlay JA 2008 *Proc. Natl. Acad. Sci. U. S. A.* **106** 8344.

[16] Campoccia D, Montanaro L and Arciola CR 2013 *Biomaterials* **34** 8533.

[17] Gunawan C, Teoh WY, Marquis CP and Amal R 2013 *Small* **9** 3554.

[18] Mäkelä JM, Keskinen H, Forsblom T and Keskinen J 2004 *J. Mater. Sci.* **39** 2783.

[19] Tikkanen J, Gross KA, Berndt CC, Pitkänen V, Keskinen J, Raghu S, Rajala M and Karthikeyan J 1997 *Surf. Coat. Technol.* **90** 210.

[20] Keskinen H, Mäkelä J, Aromaa M, Keskinen J, Areva S, Teixeira C, Rosenholm J, Pore V, Ritala M, Leskelä M, Raulio M, Salkinoja-Salonen M, Levänen E, Mäntylä T, 2006 *Catal. Lett.* **111** 127.

[21] Mäkelä JM, Aromaa M, Teisala H, Tuominen M, Stepien M, Saarinen JJ, Toivakka M, Kuusipalo J 2011 *Aerosol Sci. Technol.* **45** 827.

[22] Campoccia D, Montanaro L and Arciola CR 2013 *Biomaterials* **34** 8533.

[23] National Institute of Standards and Technology 2012 *NIST X-ray Photoelectron Spectroscopy Database version 4.1* (NIST, Gaithersburg).

[24] Biesinger MC, Lau LWM, Gerson AR and Smart RSC 2010 *Appl. Surf. Sci.* **257** 887.

[25] Chen T and Liu Y 2016 *Semiconductor Nanocrystals and Metal Nanoparticles: Physical Properties and Device Applications* (CRC Press, Boca Raton)

[26] Brobbey KJ, Haapnen J, Gunell M, Toivakka M, Mäkelä JM, Eerola E, Ali R, Saleem MR, Honkanen S, Bobacka J and Saarinen JJ 2018 *Thin Solid Films* **645** 166.

[27] Xing Y, Li X, Zhang L, Xu Q, Che Z, Li W, Bai Y and Li K 2012 *Prog. Org. Coat.* **73** 219.

[28] Joost U, Juganson K, Visnapuu M, Mortimer M, Kahru A, Nommiste E, Joost U, Kisand V and Ivask A 2015 *J. Photochem. Photobiol. B* ***142*** *178.*

[29] Brobbey KJ, Haapanen J, Mäkelä JM, Gunell M, Eerola E, Rosqvist E, Peltonen J, Tuominen M, Saarinen JJ and Toivakka M 2019 *Thin Solid Films* In press, Accepted manuscript [https://doi.org/10.1016/j.tsf.2018.12.049].

[30] Djurišić AB, Leung YH, Ng AMC, Xu XY, Lee PKH, Degger N and Wu RSS, 2015 *Small* **11** 26.

[31] Xiu Z, Zhang Q, Puppala HL, Colvin VL and Alvarez PJJ 2012 *Nano Lett.* **12** 4271.

[32] Zawadzka K, Kadziola K, Felczak A, Wronska N, Piwonski I, Kisielewska A and Lisowska K 2014 *New J. Chem.* **38** 3275.